Published in final edited form as:
Dalton Trans. 2013 March 7; 42(9): 3176–3180. doi:10.1039/c2dt32462h.

Photoluminescent DNA binding and cytotoxic activity of a platinum(II) complex bearing a tetradentate β-diketiminate ligand†

Jennifer M. Hope, **Justin J. Wilson**, and **Stephen J. Lippard**
Department of Chemistry, Massachusetts Institute of Technology, Cambridge, MA 02139, USA. Fax: +1-617-258-8150; Tel: +1-617-253-1892

Stephen J. Lippard: lippard@mit.edu

Abstract

A platinum(II) complex of a monoanionic, tetradentate β-diketiminate (BDI) ligand with pendant quinoline arms, $BDI^{QQ}H$, is reported. The complex, $[Pt(BDI^{QQ})]Cl$, is emissive in DMSO, but non-emissive in aqueous buffer. Upon binding DNA in buffer, however, a 150-fold turn-on in emission intensity occurs. Dynamic light scattering and ^1H NMR spectroscopy indicate that $[Pt(BDI^{QQ})]Cl$ forms non-emissive aggregates in aqueous solution; DNA-binding disperses the aggregates leading to the large emission turn-on response. The cytotoxic activity of the complex, measured in two cancer cell lines, is comparable to or better than that of the established anticancer drug cisplatin.

Second and third row transition metals ions with d^8 electronic configurations prefer square-planar coordination. Complexes of these ions utilizing planar, π-conjugated ligands like 2,2′-bipyridine (bpy) and terpyridine (terpy) exhibit interesting photophysical and biological properties. The low energy metal-to-ligand charge transfer (MLCT) transitions and long excited state lifetimes of these complexes render them valuable for photosensitization applications,[1–3] whereas their planar structures and cationic charges make them high-affnity DNA-metallointercalators.[4–6] The ability to intercalate into DNA can give rise to anticancer activity for certain members of this class of compounds.[7,8]

Here, we sought to investigate the photophysical and biological properties of a platinum(II) complex bearing the tetradentate, β-diketiminate ligand, $(BDI^{QQ})^-$, shown in Scheme 1. Although its synthesis was reported over 40 years ago,[9] the coordination chemistry of this ligand and its derivatives has only recently been explored;[10–12] no complexes of second or third row d^8 transition metals have yet been reported. We envisioned that this flat, tetradentate ligand would form a stable square-planar platinum(II) complex which, like those of terpyridine,[13,14] would display interesting photophysical properties, interact with DNA, and possibly induce cytotoxicity. Here we report the synthesis, characterization, and crystal structure of $[Pt(BDI^{QQ})]Cl$, its photophysical and DNA-binding properties, and its biological activity in two cancer cell lines.

The synthesis of the desired platinum(II) complex of $BDI^{QQ}H$ was carried out as indicated in Scheme 1. Two different precursors were employed. For both, the ligand was first

†Electronic supplementary information (ESI) available: Detailed experimental procedures, X-ray crystallographic data in CIF format, computational details, and additional spectroscopic studies. CCDC 905827. For ESI and crystallographic data in CIF or other electronic format see DOI: 10.1039/c2dt32462h

Correspondence to: Stephen J. Lippard, lippard@mit.edu.

deprotonated with triethylamine in acetonitrile to form a homogeneous orange solution. Treatment with either *cis*-[Pt(DMSO)$_2$Cl$_2$] or *cis*/*trans*-[Pt(SMe$_2$)$_2$Cl$_2$] resulted in precipitation of a brick-red solid. Following recrystallization of this solid by slow vapor diffusion of diethyl ether into a methanol solution, dark purple needles of the desired compound, [Pt(BDI^{QQ})]Cl, were obtained in approximately 30% yield as a dihydrate (see ESI† for details). In addition to elemental analysis and infrared (IR) spectroscopy, the complex was characterized by electrospray ionization mass spectrometry (ESI-MS), which displayed a single molecular ion peak at *m*/*z* 517.9 (Fig. S1, ESI†) corresponding to the expected complex cation [Pt(BDI^{QQ})]$^+$ (calc. *m*/*z* 518.1). ^{1}H NMR spectroscopy in DMSO-d$_6$ revealed the expected resonances for the complex, which were assigned using 2-D COSY techniques (Fig. S2 and S3, ESI†). The limited solubility of [Pt(BDI^{QQ})]Cl in DMSO and other solvents prevented acquisition of ^{13}C and ^{195}Pt NMR spectra. Cyclic voltammetry revealed the presence of two quasi-reversible reductions centred at −1.55 and −1.77 mV and an irreversible oxidation at 0.55 mV (E_p) *vs.* Fc/Fc$^+$ (Fig. S4, ESI†). By analogy to platinum(II) complexes of terpy,[15] the reduction features are assigned as ligand-based redox events, whereas the irreversible oxidation is assigned to the Pt(II)/Pt(IV) couple.

Crystals of [Pt(BDI^{QQ})]$^+$ suitable for X-ray diffraction studies were grown by vapor diffusion of diethyl ether into a DMF solution. The structure of [Pt(BDI^{QQ})]$^+$ is shown in Fig. 1; refinement and structural details are in the ESI (Tables S1 and S2†). The (BDI^{QQ})$^-$ ligand binds in a tetradentate manner, similar to that observed for the quaterpyridine ligand (QP) in the platinum(II) complex, [Pt(QP)]$^{2+}$.[16] The Pt–N distances to the quinoline rings (2.039(5) and 2.049(6) Å) are marginally longer than those to the β-diketiminate backbone nitrogen atoms (1.990(5) and 2.000(5) Å). The cation deviates slightly from planarity; the dihedral angle between the best planes defined by the quinoline rings is 12.1°. For square pyramidal Cu(II) and Zn(II) complexes of this ligand, these dihedral angles are 25.0 and 18.4°, respectively.[11] The smaller degree of ligand distortion in the platinum complex is consistent with previous computational studies indicating that BDI^{QQ} is better suited for binding to larger second and third row transition metals.[11] The [Pt(BDI^{QQ})]$^+$ cations propagate about a 2$_1$-screw axis down the crystallographic *b*-direction forming columns (Fig. 1, right). The platinum atoms of neighboring cations are offset such that the intermolecular Pt–Pt separations are 3.60 Å and the Pt–Pt–Pt angle is 140.4°. These values indicate that no direct Pt–Pt interactions are present in the lattice. The intermolecular distance between the best planes defined by the ligand chelate ring, however, is only 3.25 Å, reflecting significant π–π stacking interactions.

The spectroscopic properties of the complex are summarized in Table 1. In DMSO, the complex exhibits an intense absorption band at 342 nm along with lower-energy features at 518 nm and 546 nm. The intensity of the latter transition is somewhat greater than expected for a pure MLCT ($\varepsilon \approx$ 10 000–15 000 M^{-1} cm^{-1}). Time-dependent DFT calculations were carried out in order to gain a better understanding of these absorbance features. The calculated UV-Vis spectrum superimposed on the experimental one with electron density difference maps (EDDMs) of selected excited states is shown in Fig. 2. The EDDMs of these low energy excited states exhibit mixed MLCT and L π–π* character. The π–π* component of the lowest energy transition most likely contributes to its large extinction coeffcient. Excitation of the complex into the low-energy band gives rise to a broad emission feature centred at 672 nm (Fig. S5, ESI†). Both the intensity and lifetime of the emission depend on the presence of dioxygen in solution. In the absence of O$_2$, the quantum yield increases from 0.11 to 1.7%, and the lifetime increases from 0.68 to 6.9 μs (Fig. S6

†Electronic supplementary information (ESI) available: Detailed experimental procedures, X-ray crystallographic data in CIF format, computational details, and additional spectroscopic studies. CCDC 905827. For ESI and crystallographic data in CIF or other electronic format see DOI: 10.1039/c2dt32462h

and S7, ESI†). The large Stoke's shift, long emission lifetime, and sensitivity to the presence of oxygen are consistent with the emission arising from a triplet excited state, which is populated by intersystem crossing facilitated by the large spin–orbit coupling of the heavy platinum atom. DFT calculations predict the lowest energy triplet state to occur at 674 nm for the vertical transition or 718 nm after nuclear relaxation, consistent with the assignment of this emission as triplet-based. In aqueous buffer, the spectroscopic properties of [Pt(BDI^{QQ})]Cl are significantly different. The low-energy region of the absorption spectrum in buffer shows two peaks of roughly equal intensity at 563 and 541 nm, as well as another band at 428 nm (Fig. 2, red). The intensities of all transitions in aqueous buffer are approximately four times less than those observed in DMSO. Furthermore, the complex is effectively non-emissive; from the very weak emission that was observed, an upper limit to the quantum yield was estimated to be 0.01%, even in the absence of dioxygen (Fig. S8, ESI†).

Because many planar cationic platinum complexes bind DNA, the interaction of the [Pt(BDI^{QQ})]$^+$ cation with calf-thymus DNA (CT-DNA) in aqueous buffer was probed by UV-vis and emission spectroscopy. The addition of CT-DNA to a solution of the platinum complex in aqueous buffer led to significant spectral changes over a period of 2–3 h, indicating that the interaction between [Pt(BDI^{QQ})]$^+$ and DNA is slow to reach equilibrium. The UV-vis and emission spectra displaying these spectra at increasing DNA concentrations after overnight equilibration are shown in Fig. 3. At low (<20) DNA: Pt ratios, the absorbance band near 428 nm first increases in intensity. At higher ratios, this band continually decreases in intensity. The low energy features at 563 and 541 nm increase significantly in intensity and shift to 560 and 530 nm as DNA is added. Using a weak DNA-binding model,[17] the changes in the UV-vis spectra were fit to afford an apparent binding constant of $4.9 \pm 1.6 \times 10^3$ M^{-1}. Upon interacting with DNA, [Pt(BDI^{QQ})]$^+$ becomes emissive. The emission maximum occurs at 683 nm, slightly lower energy than that observed in DMSO. In the fully DNA-bound state, the emission quantum yield is 0.38% and the turn-on response, based on integrated emission intensity, is approximately 150. Hence, this complex is a new addition to the growing family of metal complexes that behave as DNA "light-switches".[18–25] The lifetime data of the emission in the fully bound form were best fit to a biexponential function, giving rise to two distinct values of 6.1 and 0.16 μs (Fig. S9, ESI†). These two lifetimes may correspond to different DNA-binding modes of the complex; the shorter lifetime most likely corresponds to a surface (groove) bound species that is susceptible to quenching by dioxygen. To test whether this turn-on response was selective for DNA over other macromolecules, the complex was treated with bovine serum albumin, as a model protein, and polyvinylsulfonic acid, as a generic anionic polymer. Neither of these macromolecules induced a turn-on response (Fig. S10, ESI†), thereby indicating that the complex may exhibit selectivity for DNA.

The planar cationic structure of [Pt(BDI^{QQ})]$^+$ suggests that this complex may act as an intercalating agent. Metallointercalators, however, exclusively exhibit hypochromicity upon DNA binding,[26] in contrast to the large hyperchromic effect observed for [Pt(BDI^{QQ})]$^+$ in buffer. Furthermore, binding constants for intercalating agents are typically 10^5–10^6 M^{-1}, several orders of magnitude larger than that measured for [Pt(BDI^{QQ}]$^+$. Our results therefore do not clearly point to an intercalative DNA-binding mode for [Pt(BDI^{QQ})]$^+$. A comparison of the UV-vis spectra of equal concentration solutions of [Pt(BDI^{QQ})]$^+$ in the presence of 500 equiv. of DNA in buffer *vs.* DMSO in the absence of DNA, however (Fig. S11, ESI†), reveals that the main bands in the DNA-buffer system are diminished in intensity and red-shifted relative to those in DMSO, features that are consistent with an intercalative interaction. A possible reason for the unexpected hyperchromic shift in the UV-vis spectrum and low binding affnity of the complex to DNA in buffer might be a tendency of the complex to aggregate in aqueous solution. Self-aggregation would compete with DNA

binding, giving rise to the low observed binding constant, and could also decrease the UV-vis absorbance of the complex in the absence of DNA. Aggregation is a well-documented phenomenon for related Pt-terpy complexes and metalloporphyrins.[27–32]

The aggregation of $[Pt(BDI^{QQ})]^+$ in DMSO was first investigated. Variable-concentration and -temperature ^1H NMR spectra of $[Pt(BDI^{QQ})]^+$ were acquired in DMSO-d_6. Upon increasing the temperature or decreasing the concentration, the chemical shifts systematically shifted downfield (Fig. S12, ESI†), indicating that aggregation, which depends on both these parameters, occurs to a certain extent in this solvent. In D_2O, the ^1H NMR spectrum displays broad, ill-defined peaks in the 7.5 to 5.8 ppm region (Fig. S13, ESI†), in contrast to the sharp, well resolved signals observed for all concentrations tested in DMSO-d_6. The significant broadening of the peaks in D_2O may be attributed to an increase in rotational correlation time due to the formation of large intermolecular aggregates. The aggregation of $[Pt(BDI^{QQ})]^+$ in buffer was further probed by dynamic light scattering (DLS). Buffer solutions containing $[Pt(BDI^{QQ})]^+$ effectively scattered light, enabling the measurement of average diffusion coeffcients by this method. The average diffusion coeffcient varied as a function of concentration; more concentrated samples gave rise to smaller diffusion coeffcients and *vice versa* (Fig. S14, ESI†). For the most concentrated sample (0.52 mM), the average diffusion coeffcient was measured to be 2.04×10^{-11} m^2 s^{-1}. Because DMSO solutions of $[Pt(BDI^{QQ})]^+$ did not scatter light, DLS could not be used for measuring the diffusion coeffcient. Instead, 2-D DOSY NMR spectroscopy was employed. At 1.1 mM concentration and 25 °C, the diffusion coeffcient measured by DOSY is 1.53×10^{-10} m^2 s^{-1} (Fig. S15, ESI†). Even though the viscosity of DMSO is almost twice that of water, the diffusion coeffcient measured in the former solvent is almost an order of magnitude larger than that in buffer. These data indicate that $[Pt(BDI^{QQ})]^+$ forms much higher order aggregates in aqueous compared to DMSO solutions.

Because the degree of aggregation varies with the temperature, the temperature dependence of the spectroscopic properties of $[Pt(BDI^{QQ})]^+$ were investigated. In DMSO, increasing the temperature of the solution led to a slight decrease in absorbance and a significant decrease in emission (Fig. S16, ESI†). The latter is expected for triplet states because higher temperatures favor thermal relaxation of the excited state. In aqueous buffer, increasing the temperature resulted in a hyperchromic shift of absorbance, consistent with a decrease in aggregation. Unexpectedly, the emission intensity increased significantly with increasing temperature (Fig. S17, ESI†). These results suggest that the low emission of the complex in aqueous buffers is due to the formation of non-emissive aggregates. As the temperature is increased and the presence of monomers or lower-order aggregates is favored, the emission is restored. In light of these results, which indicate a strong propensity of $[Pt(BDI^{QQ})]^+$ to aggregate in aqueous solution, the low apparent binding constant of the platinum complex to DNA may arise from competition for the formation of intermolecular aggregates. Additionally, the hyperchromic shift of the UV-vis spectrum and dramatic increase in emission intensity may occur as the large aggregates are dispersed upon DNA binding.

Because molecules that interact with DNA, including related platinum-terpy complexes, often exhibit cytotoxic properties,[33–36] the cell killing ability of $[Pt(BDI^{QQ})]^+$ was assessed in human lung carcinoma (A549) and cervical cancer (HeLa) cell lines and compared to that of the established anticancer drug cisplatin. The IC_{50} values, determined by the colorimetric MTT assay, are summarized in Table 2. These results show that $[Pt(BDI^{QQ})]^+$ exhibits cytotoxicity in HeLa cells similar to that of cisplatin, whereas in A549 cells it is approximately four times more potent. Although these studies show that $[Pt(BDI^{QQ})]^+$ is cytotoxic, the mechanism of its cytotoxic activity remains to be determined.

Conclusions

A new Pt(II) complex of the $BDI^{QQ}H$ ligand was prepared and characterized. Through spectroscopic experiments, we devised a tentative model for the behavior of this complex in solution as well as an explanation for its unusual spectroscopic properties in the presence of DNA. Although the precise mode of DNA-binding remains unclear, the emission turn-on may be useful for future cellular imaging studies. The complex also exhibits cytotoxicity comparable to or better than that of cis-platin in the two cell lines tested. Given these results, it may be of value to expand the panel of cell lines to include more cancer cell types as well as non-cancerous cells in order to further evaluate the complex as a chemotherapeutic agent.

Supplementary Material

Refer to Web version on PubMed Central for supplementary material.

Acknowledgments

This work was funded by the National Cancer Institute under Grant number CA034992. NMR equipment in the Department of Chemistry Instrumentation Facility were purchased with support from the NIH under grant number 1S10RR13886. J.M.H. and J.J.W. are grateful for partial financial support received from the MIT Undergraduate Research Opportunity Program (UROP) and a David H. Koch Graduate Fellowship, respectively. Ms. Christina J. Hanson and Dr Robert J. Radford are thanked for assistance with emission lifetime and DLS measurements, respectively, as well as for helpful discussions.

Notes and references

1. Bailey JA, Hill MG, Marsh RE, Miskowski VM, Schaefer WP, Gray HB. Inorg Chem. 1995; 34:4591.
2. Connick WB, Henling LM, Marsh RE, Gray HB. Inorg Chem. 1996; 35:6261.
3. Lai SW, Che CM. Top Curr Chem. 2004; 241:27.
4. Jennette KW, Lippard SJ, Vassiliades GA, Bauer WR. Proc Natl Acad Sci U S A. 1974; 71:3839. [PubMed: 4530265]
5. Howe-Grant M, Wu KC, Bauer WR, Lippard SJ. Biochemistry. 1976; 15:4339. [PubMed: 963039]
6. Lippard SJ, Bond PJ, Wu KC, Bauer WR. Science. 1976; 194:726. [PubMed: 982037]
7. Moretto J, Chauffert B, Ghiringhelli F, Aldrich-Wright JR, Bouyer F. Invest New Drugs. 2011; 29:1164. [PubMed: 20535526]
8. Liu HK, Sadler PJ. Acc Chem Res. 2011; 44:349. [PubMed: 21446672]
9. Zatka V, Holzbecher J, Ryan DE. Anal Chim Acta. 1971; 55:273.
10. Fritsch JM, Thoreson KA, McNeill K. Dalton Trans. 2006:4814. [PubMed: 17033706]
11. Marlier EE, Sadowsky D, Cramer CJ, McNeill K. Inorg Chim Acta. 2011; 369:173.
12. Chatelain L, Mougel V, Pécaut J, Mazzanti M. Chem Sci. 2012; 3:1075.
13. Cummings SD. Coord Chem Rev. 2009; 253:449.
14. Cummings SD. Coord Chem Rev. 2009; 253:1495.
15. Eryazici I, Moorefield CN, Newkome GR. Chem Rev. 2008; 108:1834. [PubMed: 18543874]
16. Chan CW, Che CM, Cheng MC, Wang Y. Inorg Chem. 1992; 31:4874.
17. Smith SR, Neyhart GA, Kalsbeck WA, Thorp HH. New J Chem. 1994; 18:397.
18. Friedman AE, Chambron JC, Sauvage JP, Turro NJ, Barton JK. J Am Chem Soc. 1990; 112:4960.
19. Liu HQ, Peng SM, Che CM. J Chem Soc, Chem Commun. 1995:509.
20. Liu H-Q, Cheung T-C, Che C-M. Chem Commun. 1996:1039.
21. Zhang QL, Liu JH, Ren XZ, Xu H, Huang Y, Liu JZ, Ji LN. J Inorg Biochem. 2003; 95:194. [PubMed: 12763664]
22. Liu Y, Chouai A, Degtyareva NN, Lutterman DA, Dunbar KR, Turro C. J Am Chem Soc. 2005; 127:10796. [PubMed: 16076162]

23. Lutterman DA, Chouai A, Liu Y, Sun Y, Stewart CD, Dunbar KR, Turro C. J Am Chem Soc. 2008; 130:1163. [PubMed: 18179207]
24. Stewart DJ, Fanwick PE, McMillin DR. Inorg Chem. 2010; 49:6814. [PubMed: 20593811]
25. Trovato E, Di Pietro ML, Puntoriero F. Eur J Inorg Chem. 2012:3984.
26. Long EC, Barton JK. Acc Chem Res. 1990; 23:271.
27. Jennette KW, Gill JT, Sadownick JA, Lippard SJ. J Am Chem Soc. 1976; 98:6159.
28. Mallamace F, Micali N, Scolaro LM, Pasternack RF, Romeo A, Terracina A, Trusso S. J Mol Struct. 1996; 383:255.
29. Gandini SCM, Borissevitch IE, Perussi JR, Imasato H, Tabak M. J Lumin. 1998; 78:53.
30. Casamento M, Arena GE, Lo Passo C, Pernice I, Romeo A, Scolaro LM. Inorg Chim Acta. 1998; 275–276:242.
31. Kano K, Fukuda K, Wakami H, Nishiyabu R, Pasternack RF. J Am Chem Soc. 2000; 122:7494.
32. Krause-Heuer AM, Wheate NJ, Price WS, Aldrich-Wright J. Chem Commun. 2009:1210.
33. McFadyen WD, Wakelin LPG, Roos IAG, Leopold VA. J Med Chem. 1985; 28:1113. [PubMed: 4020833]
34. Lowe G, Droz AS, Vilaivan T, Weaver GW, Park JJ, Pratt JM, Tweedale L, Kelland LR. J Med Chem. 1999; 42:3167. [PubMed: 10447962]
35. Ma DL, Che CM. Chem– Eur J. 2003; 9:6133. [PubMed: 14679525]
36. Ma D-L, Shum TY-T, Zhang F, Che C-M, Yang M. Chem Commun. 2005:4675.

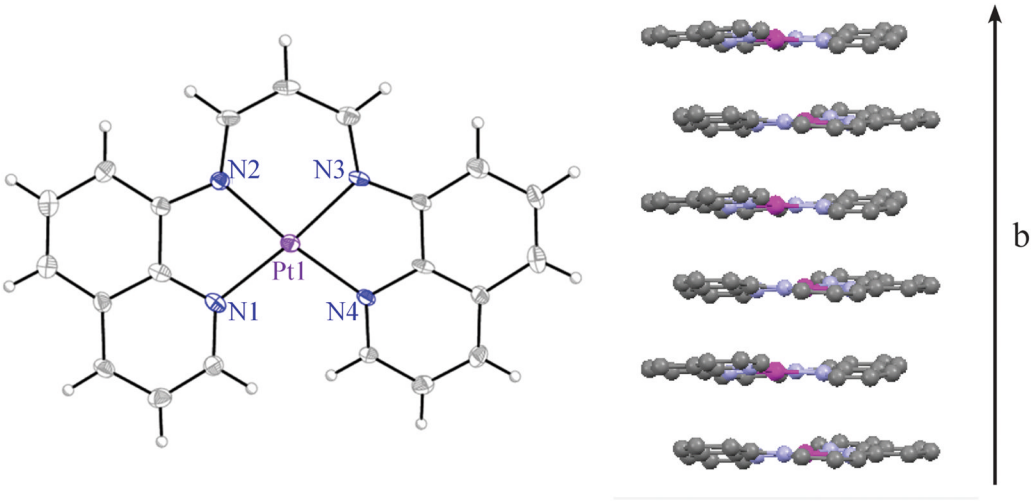

Fig. 1.

X-ray crystal structure of $[Pt(BDI^{QQ})]^{+}$ (left). Ellipsoids are drawn at the 50% probability level. Unlabeled grey and white ellipsoids correspond to carbon and hydrogen atoms, respectively. Intermolecular stacking interaction observed in the crystal lattice (right).

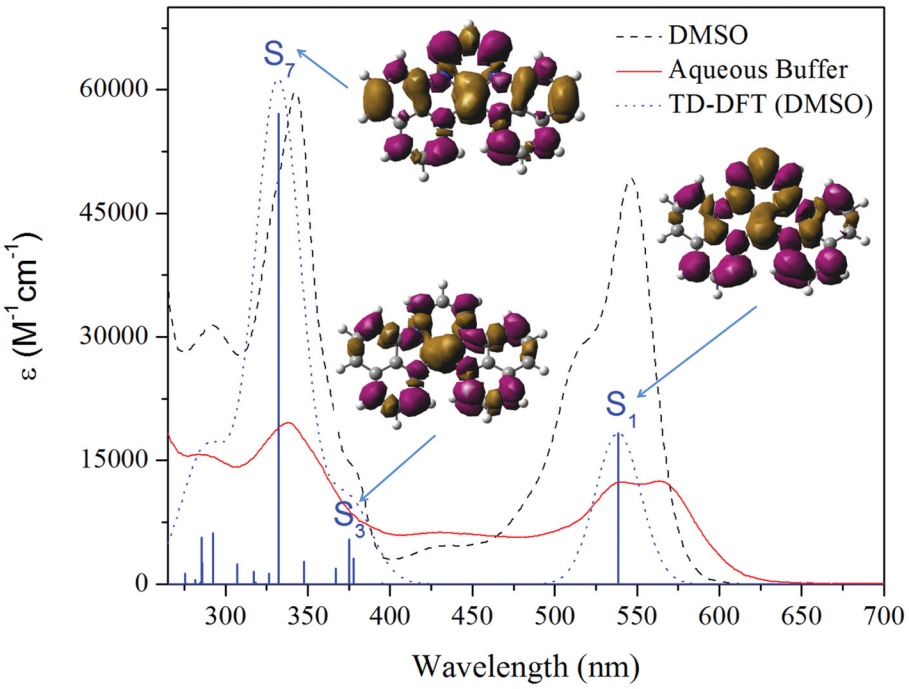

Fig. 2.

UV-vis spectra of [Pt(BDI^{QQ})]Cl in DMSO (black, dashed) and aqueous buffer (red, solid, pH 7.4, 10 mM Tris, 10 mM NaCl). The dotted blue line is the simulated UV-vis spectrum from TD-DFT calculations with a DMSO solvation model. The solid blue bars represent individual singlet transitions, and the associated EDDMs for selected transitions are displayed.

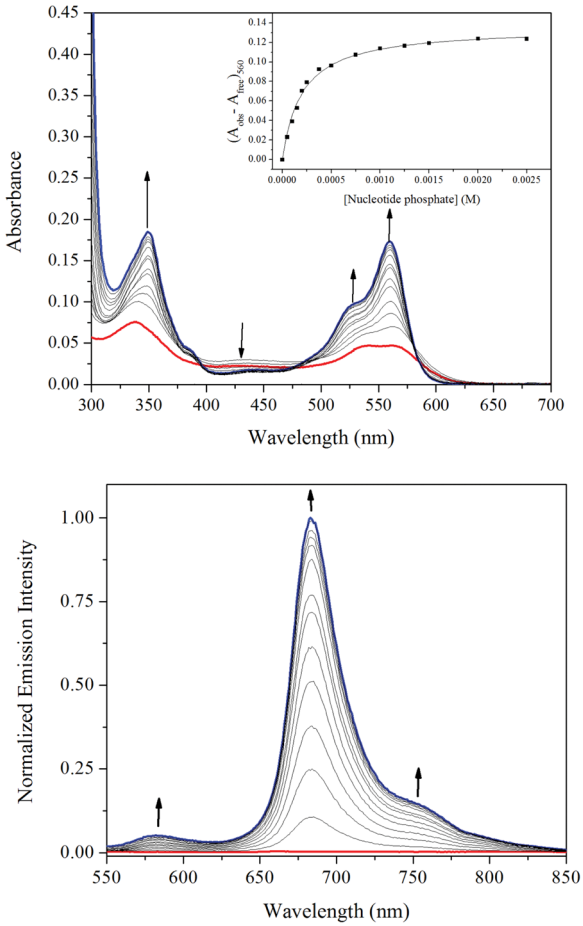

Fig. 3.

UV-vis (top) and emission (bottom) spectral changes of [Pt(BDI^{QQ})]Cl upon the addition of up to 500 equiv. nucleotide of CT-DNA in buffer (pH 7.4, 10 mM Tris, 10 mM NaCl) after a 16 h equilibration period. The black arrows mark the spectral changes as the concentration of CT-DNA increases. The inset shows a plot of [DNA] *vs.* absorbance at 560 nm.

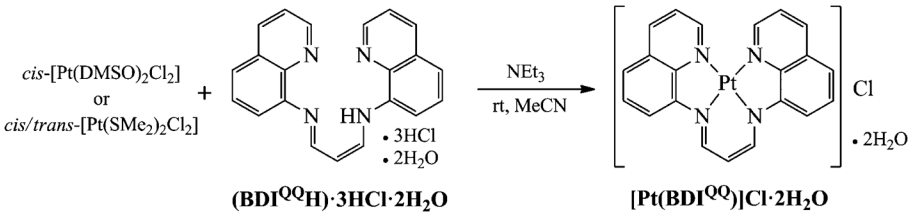

(BDI^{QQ}H)·3HCl·2H$_2$O **[Pt(BDI^{QQ})]Cl·2H$_2$O**

Scheme 1.
Synthesis of [Pt(BDI^{QQ})]Cl.

Table 1

Spectroscopic properties of [Pt(BDI^{QQ})]Cl

Solvent	λ_{max}, nm (ε, M^{-1} cm^{-1})	λ_{em}, nm (Φ)[b]	τ_{em} (μs)
DMSO	292 (29 000), 342 (60 000), 377 (14 000), 434 (4700), 518 sh (29 000), 546 (49 000)	Presence of O_2: 672 (1.1×10^{-3})	Presence of O_2: 0.68
		Absence of O_2: 672 (1.7×10^{-2})	Absence of O_2: 6.9
Aqueous buffer[a]	284 (15 000), 338 (19 000), 428 (6100), 541 (12 000), 563 (12 000)	No DNA: 720, 820 ($<1 \times 10^{-4}$)	No DNA: n.d.
		Excess DNA: 682 (3.8×10^{-3})	Excess DNA: 0.16, 6.1

[a] pH 7.4, 10 mM Tris, 10 mM NaCl.

[b] Measured relative to $[Ru(bpy)_3]^{2+}$ in aerated water ($\Phi = 0.04$).

Table 2

Cytotoxicity of [Pt(BDI^{QQ})]Cl and cisplatin

	IC_{50} (μM)	
Compound	**HeLa**	**A549**
Cisplatin	2.3 ± 1.4	5.2 ± 1.0
[Pt(BDI^{QQ})]Cl	2.8 ± 1.7	1.2 ± 0.2